

The rubber tree genome reveals new insights into rubber production and species adaptation

Chaorong Tang^{1†*}, Meng Yang^{2,3†}, Yongjun Fang^{1†}, Yingfeng Luo^{2†}, Shenghan Gao², Xiaohu Xiao¹, Zewei An¹, Binhui Zhou^{1,4}, Bing Zhang⁵, Xinyu Tan², Hoong-Yeet Yeang⁶, Yunxia Qin¹, Jianghua Yang¹, Qiang Lin², Hailiang Mei^{2,3}, Pascal Montoro⁷, Xiangyu Long¹, Jiyan Qi¹, Yuwei Hua¹, Zilong He^{2,3}, Min Sun⁵, Wenjie Li⁵, Xia Zeng¹, Han Cheng¹, Ying Liu⁵, Jin Yang⁵, Weimin Tian¹, Nansheng Zhuang⁴, Rizhong Zeng¹, Dejun Li¹, Peng He¹, Zhe Li¹, Zhi Zou¹, Shuangli Li⁵, Chenji Li², Jixiang Wang², Dong Wei², Chao-Qiang Lai⁸, Wei Luo¹, Jun Yu^{2*}, Songnian Hu^{2,3*} and Huasun Huang^{1*}

The Para rubber tree (*Hevea brasiliensis*) is an economically important tropical tree species that produces natural rubber, an essential industrial raw material. Here we present a high-quality genome assembly of this species (1.37 Gb, scaffold N50 = 1.28 Mb) that covers 93.8% of the genome (1.47 Gb) and harbours 43,792 predicted protein-coding genes. A striking expansion of the REF/SRPP (rubber elongation factor/small rubber particle protein) gene family and its divergence into several laticifer-specific isoforms seem crucial for rubber biosynthesis. The REF/SRPP family has isoforms with sizes similar to or larger than SRPP1 (204 amino acids) in 17 other plants examined, but no isoforms with similar sizes to REF1 (138 amino acids), the predominant molecular variant. A pivotal point in *Hevea* evolution was the emergence of REF1, which is located on the surface of large rubber particles that account for 93% of rubber in the latex (despite constituting only 6% of total rubber particles, large and small). The stringent control of ethylene synthesis under active ethylene signalling and response in laticifers resolves a longstanding mystery of ethylene stimulation in rubber production. Our study, which includes the re-sequencing of five other *Hevea* cultivars and extensive RNA-seq data, provides a valuable resource for functional genomics and tools for breeding elite *Hevea* cultivars.

The rubber tree (*Hevea brasiliensis*, hereafter referred to as *Hevea*) is a member of the spurge family (Euphorbiaceae), along with several other economically important species such as cassava (*Manihot esculenta*) and the castor oil plant (*Ricinus communis*). Natural rubber (*cis*-1, 4-polyisoprene) makes up about one-third of the volume of latex that is essentially cytoplasm of the articulated laticifers in *Hevea*. The latex is extracted by tapping the bark, a non-destructive method of harvesting that facilitates continual production. As an industrial commodity, natural rubber is an elastomer with physical and chemical properties that cannot be fully matched by synthetic rubber¹. In contrast to synthetics, the production of natural rubber is sustainable and environment friendly². The commercial cultivation of *Hevea*, a native to the Amazon Basin, began in 1896 on a plantation scale in Malaya (now Malaysia) and expanded to other Southeast Asian countries that lead in world natural rubber production today³. Decades of selective breeding have resulted in a gradual improvement in rubber productivity, from 650 kg ha⁻¹ derived from unselected seedlings during the 1920s to 2,500 kg ha⁻¹ yielded by elite cultivars by the 1990s⁴. Nevertheless, the field production achieved so far is still well below the theoretical yield of 7,000–12,000 kg ha⁻¹, as has been suggested for the rubber tree⁵. Meanwhile, conventional rubber breeding has been stagnating in the introduction of high-yield cultivars. The reasons include a

narrow genetic basis for exploiting breeding potential and difficulty in introducing wild germplasm because of the genetic burden in removing unfavourable alleles⁶. The incorporation of marker-assisted selection and transgenic techniques offers promise to improve breeding efficiency for latex yield, and sequencing of the *Hevea* genome would uncover even more avenues leading to this end.

The first draft *Hevea* genome was released by a Malaysian team⁷ that was participant to the recent boom in transcriptomic and proteomic studies of the species^{8–11}. However, its low sequence coverage (~13×) and a lack of large insert libraries (such as fosmid- or BAC-based clone libraries) have limited the success of genome assembly (a scaffold N50 size of 2,972 bp), precluding its application for furthering quality research in the field.

Here, we report a high-quality genome assembly of *Hevea* Reyan7-33-97, an elite cultivar widely planted in China^{12,13} based on sequence data from both whole-genome shotgun (WGS) and pooled BAC clones. This assembly contains 7,453 scaffolds (N50 = 1.28 Mb), has a length of 1.37 Gb and covers ~94% of the predicted genome size (1.46 Gb). Together with analysis of data from re-sequencing five other cultivars and comprehensive transcriptomic surveys, we aim to obtain new insights into the physiology of laticifers and molecular details of rubber biosynthesis, especially in relation to ethylene-stimulated rubber production.

¹Rubber Research Institute, Chinese Academy of Tropical Agricultural Sciences (CATAS), Danzhou 571737, China. ²CAS Key Laboratory of Genome Sciences and Information, Beijing Institute of Genomics, Chinese Academy of Sciences (CAS), Beijing 100101, China. ³University of Chinese Academy of Sciences, Beijing, China. ⁴College of Agronomy, Hainan University, Haikou 570228, China. ⁵Core Genomic Facility, Beijing Institute of Genomics, CAS, Beijing 100101, China. ⁶Bukit Bandar Raya, 59100 Kuala Lumpur, Malaysia. ⁷CIRAD, UMR AGAP, F-34398, Montpellier, France. ⁸Nutrition and Genomics Laboratory, JM-USDA Human Nutrition Research Center on Aging, Tufts University, Massachusetts 02111, USA. [†]These authors contributed equally to this work. *e-mail: chaorongtang@126.com; yujun@big.ac.cn; husn@big.ac.cn; xjshhs@163.com

Results

Genome assembly and annotation. We assembled the *Hevea* genome (cultivar Reyan7-33-97) based on 138 Gb (94× genome coverage) processed shotgun sequences (Illumina GA2 and Hiseq 2000; Supplementary Table 1). We also generated paired-end reads for five other *Hevea* cultivars (PR107, Reyan8-79, RRIM600, Wenchang11 and Yunyan77-4) with high-coverage of 38× to 59× (Supplementary Fig. 1 and Supplementary Table 2). Based on a 17-mer sequence library, the estimated genome size of Reyan7-33-97 is 1.46 Gb, whereas that of the other five cultivars ranges from 1.41 Gb to 1.55 Gb (Supplementary Fig. 2). To assist with scaffold construction, we generated an additional 55-Gb high-quality mate-pair data (insert sizes from 800 to 10,000 bp; 682× physical coverage; Supplementary Table 1 and Supplementary Fig. 3), and obtained a preliminary assembly with a scaffold N50 value of 55 kb. We further improved the assembly by adding pooled BAC sequences (Supplementary Fig. 4 and Supplementary Note 1) from 47,616 BAC clones (mean insert size = 135 kb) (Supplementary Table 3 and Supplementary Fig. 5) that generated pseudo-mate-pair reads of 10 to 200 kb insert lengths to assist scaffolding (Supplementary Fig. 6). This yielded a 1.37-Gb genome assembly that covers 93.8% of the estimated genome size, and contains 7,453 scaffolds (N50 = 1.28 Mb) and 84,285 contigs (N50 = 30.6 kb) (Table 1).

To validate quality of the assembly, we first aligned all *Hevea* DNA, expressed sequence tag (EST) and protein sequences available in the public domain to show mapping rates of 91.5, 97.9 and 100%, respectively (Supplementary Figs 7 and 8). Of the 1.11-Gb *Hevea* genome assembled by the Malaysian group⁷, only 25.2 Mb failed to be aligned to our assembly. The unalignable portions may reflect real sequence differences between cultivars, RRIM600 used by the Malaysian team and Reyan7-33-97 in the present study, as also reflected in the genome size difference (Supplementary Fig. 2). Next, we aligned 18 BAC scaffolds with low repetitive sequences to our genome assembly, and yielded alignments from 91.69% to 99.74% (Supplementary Fig. 9). Finally, the transcripts we assembled also showed excellent alignment to the genome; of 84,241 transcripts, 98.32% were mapped (transcript coverage > 80% and identity > 99%; Supplementary Table 4 and Supplementary Note 4).

To assist genome annotation and gene expression analysis, we combined three methods: *ab initio*, 84,241 unique transcripts (Supplementary Table 5 and Supplementary Fig. 10) and protein homologues (Supplementary Fig. 11) to define 43,792 protein-coding genes (Table 1), of which 39,919 were found in the NCBI non-redundant protein database (NRPD, Mar. 2015, Supplementary Table 6). A gene family survey clustered 16,315 gene families, among which 1,077 are *Hevea* specific and 10,675 are shared with *Manihot esculenta*, *Ricinus communis*, *Populus trichocarpa* and *Linum usitatissimum* (Fig. 1a and Supplementary Note 9). In addition, a homologue search for non-coding RNAs predicted 167 ribosomal RNAs, 591 miRNAs, 10 SPARNAs, 3,445 SnoRNAs, 4 tmRNAs, 697 tRNAs, 219 snRNAs and 217 other types of RNAs (Supplementary Table 7).

Repeat-driven genome expansion. We identified 71% of the genome length as repeats (Table 1 and Supplementary Table 8). Among the five species of Malpighiales (*Hevea*, *Manihot*, *Ricinus*, *Populus* and *Linum*), *Hevea* not only has the largest genome but also the greatest repeat content (Supplementary Table 9). Of the repeat sequences, two types of long-terminal repeat retrotransposons (LTR-RTs), *Gypsy* (691,209 in number) and *Copia* (114,165), are most abundant, and they total more than half (~0.7 Gb; 50.9%) of the genome assembly, substantially higher than that of the other four Malpighiales species. Among the five Malpighiales species, *Hevea* harbours the largest set (35,079) of LTR-RTs (Supplementary Table 10), and both *Gypsy*

Table 1 | Statistics for the *Hevea* genome and gene annotation.

Estimate of genome size	1.46 Gb
Number of scaffolds	7,453
Total length of scaffolds	1.37 Gb
N50 of scaffolds	1.28 Mb
Longest scaffolds	6.41 Mb
Number of contigs	84,285
Total length of contigs	1.29 Gb
N50 of contigs	30.6 kb
Longest contigs	312.7 kb
GC content	34.84%
Number of genes	43,792
Percentage of gene length in genome	12.47%
Mean gene length	3,913 bp
Gene density	31.9 Mb ⁻¹
Transcripts number	46,631
Mean transcript length	1,483 bp
Mean coding sequence length	1,123 bp
Mean exon length	308 bp
Exons GC content	41.54%
Mean intron length	677 bp
Intron GC content	32.61%
Masked repeat sequence length	977.5 Mb
Repeats percentage of total scaffolds	71.18%
Repeats percentage of total contigs	75.69%

and *Copia* show a peak substitution rate around 0.05, suggesting a burst of LTR-RT insertion at that point (of time) (Supplementary Fig. 12), which occurred five million years (Myr) ago as calculated (see Methods). Similar to *Hevea*, three other Malpighiales species (*Manihot*, *Ricinus* and *Populus*, with *Linum* being the exception) have more *Gypsy* than *Copia*, and share nearly identical substitution rates for the two elements (Supplementary Fig. 12).

Genome duplication, collinearity and phylogeny. We explored gene-based collinearity and calculated synonymous substitution rate (K_s) as well as fourfold synonymous third-codon transversion (4DTv) rate among paralogues and orthologues. With the exception of *Ricinus*, all the other four Malpighiales species display an obvious two-peak pattern for the distributions of K_s /4DTv, with the left sharp peak representing the recent species-specific duplication and the right smooth one representing the eukaryotic duplication (Fig. 1b). The most ancient peak, representing γ duplication, is rather obscure and mingled with the right peak. A recent phylogenomic analyses inferred the clades Euphorbiaceae (*Hevea*, *Manihot*), Salicaceae (*Populus*) and Linaceae (*Linum*) to have emerged 89.9, 58.0 and 39.5 Myr ago, respectively¹⁴. Hence, *Linum* is the youngest of the five species, as also reflected by its lower K_s and 4DTv peak values (Fig. 1b). If the diversification time is assumed to a maximum of 89.9 million years, according to the K_s value of the second peak, the *Hevea* synonymous substitution constant is estimated as 7.5×10^{-9} per site per year. Thus, the recent *Hevea*-specific duplication might have occurred in ~15.3 Myr ago, nearly 10 million years earlier than the burst of *Hevea* LTR insertion. However, we are still not sure whether the two duplication events in *Hevea* are whole genome duplication because only 30.0% and 5.8% genes are covered by the first and second peaks, respectively. In comparison, the relative rates in *Manihot*, *Populus* and *Linum* are much higher; for example, 92.8% and 56.8% genes are attributable to the two peaks of *Populus* (Supplementary Table 12).

Plotting collinear regions of *Hevea* with itself and five other species reveals obvious conserved gene clusters (Supplementary Fig. 13). The absence of collinearity with *Ricinus* is unexpected, which might indicate a lack of species-specific duplication in *Ricinus* as revealed by its K_s /4DTv distribution pattern (Fig. 1b). Among *Hevea*, *Manihot* and *Populus* (Supplementary Fig. 14), the collinearity size of *Hevea* is significantly larger than that of

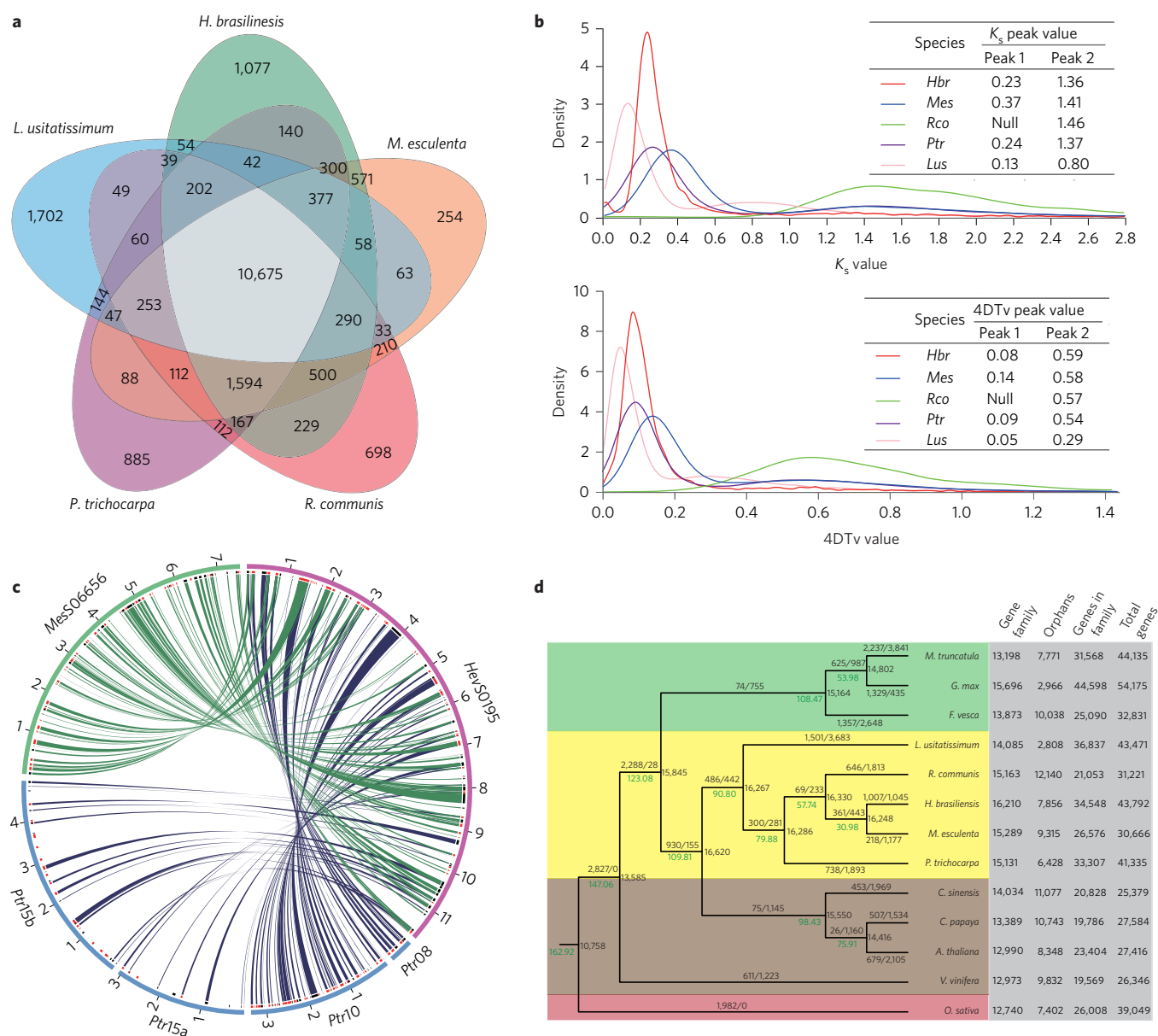


Figure 1 | Collinearity and evolution of the *Hevea* genome. **a**, A Venn diagram of shared orthologues among five species. Each number represents a gene family number. **b**, Density distributions of K_s and 4DTv for paralogous genes. The peak values are shown in insets. *Hbr*, *H. brasiliensis*; *Mes*, *M. esculenta*; *Rco*, *R. communis*; *Ptr*, *P. trichocarpa*; *Lus*, *L. usitatissimum*. **c**, Collinear region representation of *Hbr* scaffold0195 to the corresponding *Mes* and *Ptr* scaffolds. The outer circle with different colours denotes scaffolds of different species. Each scaffold is scaled, and the scale label is 1×10^{-6} of actual size. The inner circle shows the genes in the corresponding scaffolds, and genes in positive and negative strands are represented by red and black colours, respectively. The collinear blocks between two species are linked by curved ribbons. **d**, Phylogenetic tree of 13 species based on orthologues of single-gene families. The number in each node indicates the number of gene families. The number at the root (10,758) represents the number of gene families in the common ancestor. The values above each branch denote gene family gain/loss number at each round of genome duplication after diversifying from the common ancestor. The green numbers below each branch denote speculated divergent time of each node. The clades are marked by four different block colours in the tree: the last one (red) is a monocot species, *O. sativa*, used as an outgroup; the first three are Rosids clades in dicots, including Fabidae (green), COM (yellow) and Malvidae (brown). Bootstrap values for each node are above 50%.

Manihot ($P = 1.3 \times 10^{-8}$) or *Populus* ($P = 1.79 \times 10^{-7}$). The largest collinearity region exists between *Hevea* scaffold0195 (1,174,012 bp; 108 genes) and *Manihot* scaffold06656 (752,726 bp; 81 genes) (Fig. 1c), where 71 genes are overall matched. In *Populus*, four scaffolds are collinear to the *Hevea* scaffold0195, indicating structural variations between *Hevea* and *Populus*.

To analyse the gene gain–loss event, we used 72 single-copy gene families to construct a maximum likelihood phylogeny between *Hevea* and 12 other species (Fig. 1d), representing a typical Rosid clade sequenced so far in Eudicots. Taxonomically, *Hevea*,

Manihot, *Ricinus*, *Populus* and *Linum* belong to the Celastrales–Oxalidales–Malpighiales (COM). The phylogenetic placement of the COM clade remains controversial in angiosperms. Here, the COM clade was placed in Malvidae, consistent with a recent study using single- and multicopy nuclear loci¹⁵. Among the 13 species examined, *Hevea* and rice are representative of the most and fewest gene families, respectively. In most species, the gene family gain is less than gene loss; the only exceptions are in rice and soybean. The divergence time for the Euphorbiaceae family is estimated to be 57.7 Myr ago (Fig. 1d), more recent than a previously

reported dating of 89.9 Myr ago¹⁴, possibly because of the limited number of Euphorbiaceae species used here.

Genetic diversity among *Hevea* cultivars. The high-quality genome assembly allows us to characterize genetic diversity among the *Hevea* cultivars Reyan7-33-97 (RY73397), PR107, RRIM600, Wenchang11 (WC11), Reyan8-79 (RY879) and Yunyan77-4 (YY774) (Supplementary Table 2). Among them, PR107 and RRIM600 are cultivated globally, and the other four are elite cultivars bred and widely planted in China, with PR107 and/or RRIM600 as direct or indirect parents (Supplementary Fig. 1).

The density of single nucleotide polymorphisms (SNPs) contributed by all cultivars averages ~2 SNPs per kilobase (Supplementary Table 12), and 95.1–95.6% SNPs occur in non-coding regions (Supplementary Table 13). YY774 has the most variety-specific SNPs (442,278), whereas WC11 has the least (132,006) (Fig. 2a). Phylogeny based on SNPs shows the genetic relationship among the cultivars (Fig. 2b) is consistent with their breeding history (Supplementary Fig. 1).

Low genetic diversity regions or ‘SNP deserts’ often indicate selective sweeps¹⁶ and relate to domestication in many major crop species^{17,18}. All re-sequenced *Hevea* cultivars exhibit a unimodal pattern in the distribution of SNPs with a single low-SNP peak at <1 SNP per kilobase (Fig. 2b), contrasting with bimodal curves observed in rice and date palm, where the low-SNP peak reflects trait selection in cultivation^{17,19}. The SNP deserts account for 42% of the *Hevea* genome (Supplementary Table 14), a value significantly higher than that reported in rice (8%)¹⁷ or date palm (18%)¹⁹. Compared with the genome average, the SNP desert has a higher K_a/K_s (nonsynonymous/synonymous substitution) ratio (1.72 versus 1.27) (Supplementary Table 14). The low-SNP peak in various cultivars might be attributed to natural selection; artificial selection remains a possibility, although to a lesser extent due to a short domestication history of *Hevea* (since the late nineteenth century).

About half of SNP deserts (13,127 blocks, 261,150 kb) are conserved in all six cultivars (Supplementary Table 15), defined as shared or core SNP deserts representing most sequence signatures left mainly by natural selection after *Hevea* speciation. There are 3,820 genes (8.7% of the total genes) located in the core SNP desert (Supplementary Table 16) that are most enriched in respiratory electron transport chain and defence response functions (Fig. 2c). Of particular interest is the fact that the single most highly expressed gene in latex—by a wide margin—*REF1* resides in the core SNP desert (Supplementary Tables 16 and 20). In this regard, the sister gene to *REF1*, *SRPP1*, is noteworthy by its absence in the SNP desert. Meanwhile, both genes showed the least sequence diversity among the six *Hevea* cultivars examined, suggesting the importance of their conservation in this species (Supplementary Table 17).

Rubber biosynthesis and expansion of the REF/SRPP family. In the laticifer network of *Hevea*, natural rubber is synthesized by a sequential condensation of isopentenyl diphosphates (IPPs) in *cis*-configuration to the priming allylic molecules (initiators)²⁰. By convention, genes involved in the synthesis of IPP to the final rubber polymer are termed as rubber biosynthesis genes²¹. From our genome assembly, 84 rubber biosynthesis genes from 20 gene families were identified (Supplementary Table 18), including 18 in the cytosolic mevalonate (MVA) pathway and 22 in the plastidic 2-C-methyl-D-erythritol-4-phosphate (MEP) pathway for IPP synthesis, 15 for initiator synthesis in the cytosol and 39 for ‘rubber elongation’ on rubber particles (Fig. 3a). Of the 24 MEP genes, only two *DXS* (1-deoxy-D-xylulose 5-phosphate synthase) genes (*DXS7* and *DXS10*) show substantial and preferential expression in latex (Fig. 3a and Supplementary Table 18). In contrast, at least one gene for each MVA pathway enzyme shows latex-biased abundant expression, supporting the proposition that

it is the MVA rather than the MEP pathway that is involved in rubber biosynthesis^{22,23}. Three gene families, *REF/SRPP*, *CPT* (*cis*-prenyltransferase) and *DXS*, have more than ten genes. Recently, a homologue of the human Nogo-B receptor was demonstrated to be essential for rubber biosynthesis in dandelion²⁴. However, blast searching yielded no significant hits in our genome assembly or the public *Hevea* sequences, indicating a discrepancy in the mechanisms of rubber biosynthesis between these two species.

The 18-member REF/SRPP family of *Hevea* is the largest compared with the other 17 sequenced plants examined this study (10 at most) (Supplementary Table 19), indicating an obvious expansion of this family in *Hevea*. The gene number of the REF/SRPP family does not seem to correlate with either genome size or polyploidy of a given species. For example, only four REF/SRPP genes are identified in the hexaploid *Triticum aestivum* genome (17 Gb) but six in the small diploid genome of *Populus trichocarpa* (480 Mb). When considering other rubber-producing plants, eight REF/SRPP genes are identified in *Lactuca sativa* and six in limited EST/mRNA sequences of *Parthenium argentatum* (Supplementary Table 19). These results suggest a possible link between expansion of the REF/SRPP family and the ability to produce rubber.

A close involvement of REF and SRPP in rubber synthesis has been proposed based on *in vitro* rubber biosynthesis assays^{25,26}, and a positive correlation of *REF* expression with rubber yield²⁷. Recent transgenic studies in *Taraxacum brevicorniculatum*^{28,29} also reveal their essential role in rubber biosynthesis. REF and SRPP share a conserved REF motif that is also retained in several stress-related or lipid droplet-associated proteins in plant cells^{25,30,31}. Based on the presence of a carboxy (C) terminus found in SRPP and its absence in REF^{25,30}, and the similarities among protein sequences, the 18 *Hevea* REF/SRPP genes are named *SRPP1* to *10* and *REF1* to *8* (Supplementary Fig. 15). Of these, *REF1* (138 aa) and *SRPP1* (204 aa) are the two most abundant isoforms (Supplementary Table 18), and correspond, respectively, to the well characterized REF and SRPP^{25,26}. In the other 17 plants examined, the REF/SRPP family has isoforms with sizes similar to or larger than *SRPP1*, but no isoforms with similar size to *REF1*. The uniqueness of *REF1* is highlighted by an alignment of REF/SRPP proteins from different plants (Supplementary Fig. 16).

The 18 REF/SRPP genes exhibit distinct expression patterns in seven *Hevea* tissues (Fig. 3a). Four isoforms, *REF1*, *SRPP1*, *REF3* and *REF7*, have striking RPKM values of >7,000 in latex, this being especially true of *REF1* (38,999). In total they account for 96.8% of expression of the REF/SRPP gene family in latex (Supplementary Table 18). In addition, their expression in latex is over tenfold higher than in any other tissue. Considering the fact that all other tissues also contain laticifers and small amounts of latex, we think that the expression of these genes in the tissues may have arisen from latex itself, and *REF1*, *SRPP1*, *REF3* and *REF7* are thus essentially laticifer-specific genes. When compared with all the genes expressed in latex, these four REF/SRPP genes rank among the top, with *REF1* ranked first, *SRPP1* sixth, *REF3* ninth and *REF7* the twelfth (Supplementary Table 20).

Phylogenetically, the *Hevea* REF/SRPP genes are classified into two major groups, with 14 in group I and four in group II (Fig. 3b). Of the group II genes, three (*SRPP4*, *6* and *10*) are not expressed or expressed at very low levels in latex, and the remaining *SRPP7* shows somewhat constitutive low expression across different tissues (Fig. 3a), therefore precluding the active participation of group II genes in rubber biosynthesis. group I genes are further divided into two distinct clades, 13 in clade 1 and only *SRPP2* in clade 2. *SRPP2* exhibited moderate expression across diverse tissues, excluding its special function in laticifers. Interestingly, all latex-specific isoforms (*REF1*, *SRPP1*, *REF3* and *REF7*) are clustered in clade 1. When the REF/SRPPs from *Hevea* and 11 other plants were investigated for their phylogenetic relationship, all the 13

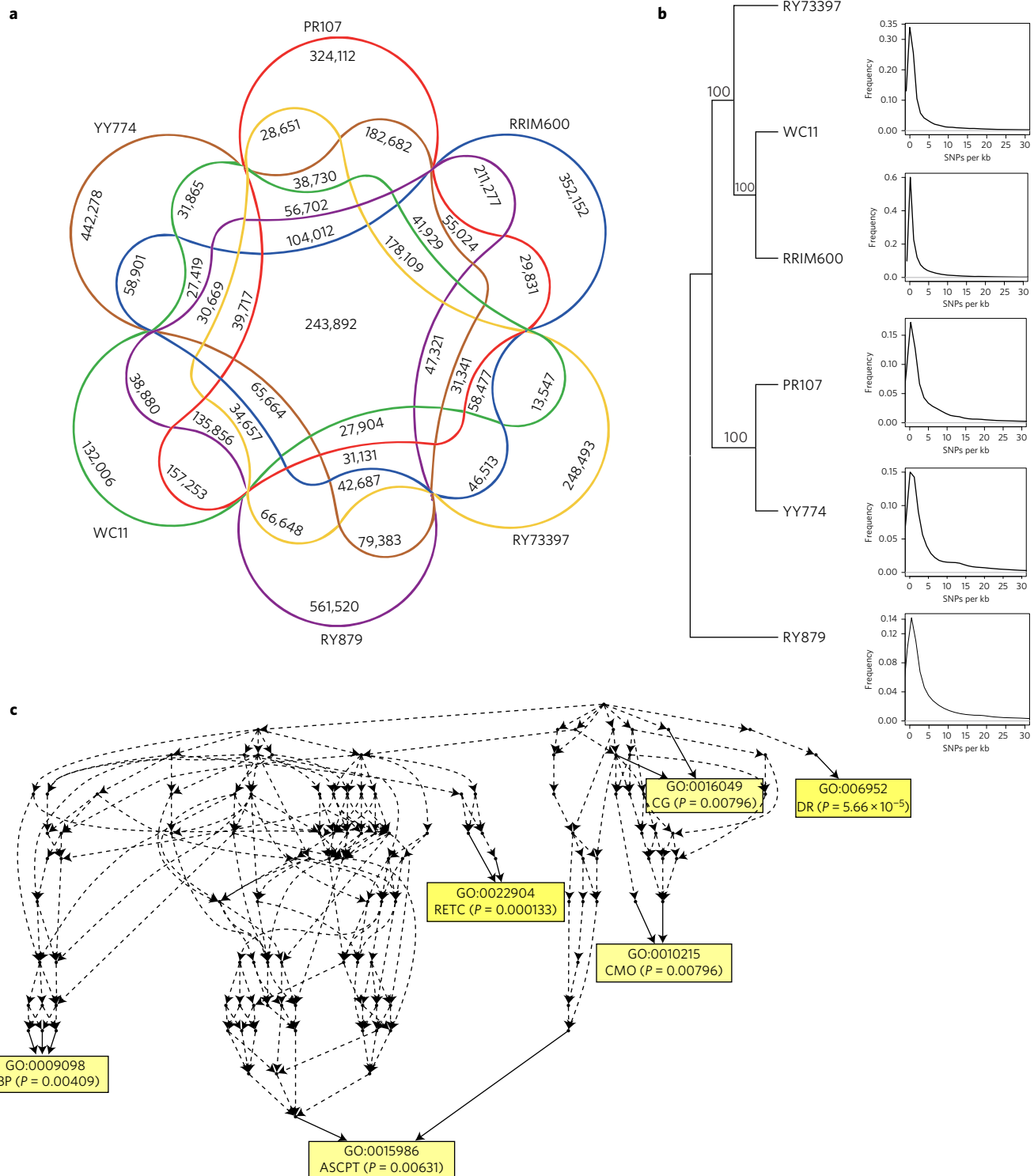


Figure 2 | Genetic diversity among six *Hevea* cultivars. **a**, SNP number distribution in six cultivars. **b**, Phylogenetic analysis of cultivars based on SNPs and frequency distribution. Using homology SNP sites of the cultivars, the tree is constructed by MEGA5.1 with the Neighbour-Joining model and the bootstrap test (1,000 replicates). The series of plots on the right show SNP density (SNP per kb) and frequencies. SNP frequency is calculated based on a 50-kb sliding window in 1-kb steps. **c**, Gene Ontology (GO) enrichment in biological process for genes located in core SNP desert using GOEAST. Note that two biological processes, defence response (DR) and respiratory electron transport chain (RETC), are most enriched. LBP, leucine biosynthetic process; ASCPT, ATP synthesis coupled proton transport; CMO, cellulose microfibril organization; CG, cell growth.

clade 1 isoforms were clustered into an independent clade whereas the remainder were scattered together with the homologues from other plants into different clades (Supplementary Fig. 17). These results suggest that the clade 1 *REF/SRPP* genes might have evolved independently towards functioning in rubber biosynthesis.

The *Hevea* REF/SRPP family was further surveyed for their genomic location. Of particular note, 12 of the 13 clade 1 REF/SRPPs including the four laticifer-specific genes, are located in a single 205-kb Scaffold1222 whereas the remaining six are scattered into six different scaffolds (Fig. 3c and Supplementary Fig. 18). *SRPPI*

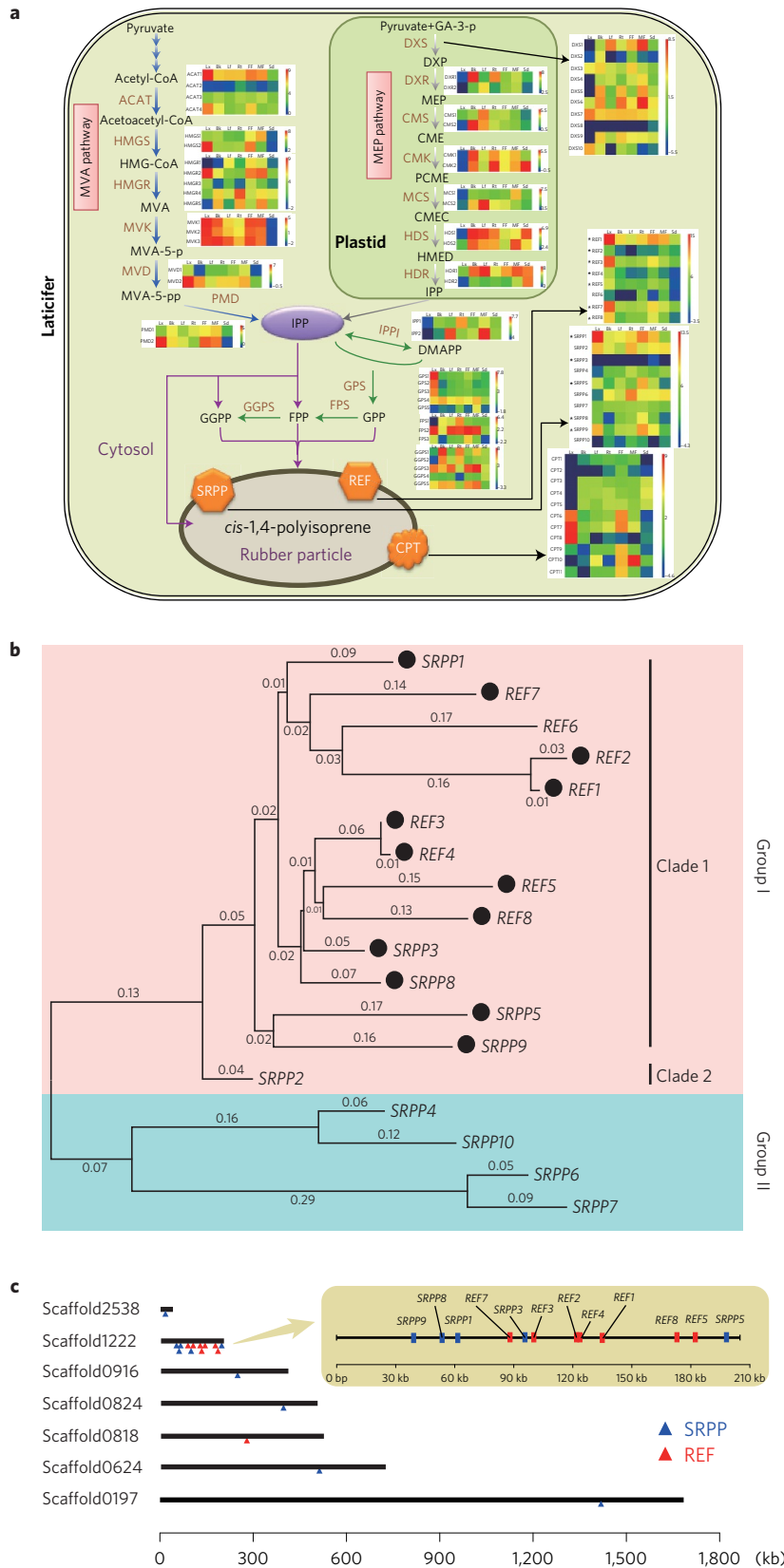


Figure 3 | Rubber biosynthesis and expansion of the REF/SRPP gene family in *Hevea*. **a**, The rubber biosynthesis pathway and expression profiles (reads per kilobase per million reads mapped; RPKM) of the genes involved in rubber biosynthesis. Lx, latex; Bk, bark; Lf, leaf; Rt, root; FF, female flower; MF, male flower. **b**, Phylogeny of the REF/SRPP gene family. Full-length coding sequences of the 18 REF/SRPPs are aligned with MAFFT v7.205. The tree is constructed by using MEGA5.1, with the Neighbour-Joining model and bootstrap test with 1,000 replicates. **c**, Genomic location of the *Hevea* REF/SRPP genes. Scaffolds are represented as solid bars on the left and length scale on the bottom. Note that most of the REF/SRPP genes, including the four laticifer-specific ones (*REF1*, *SRPP1*, *REF3* and *REF7*), are located in a single scaffold (Scaffold1222).

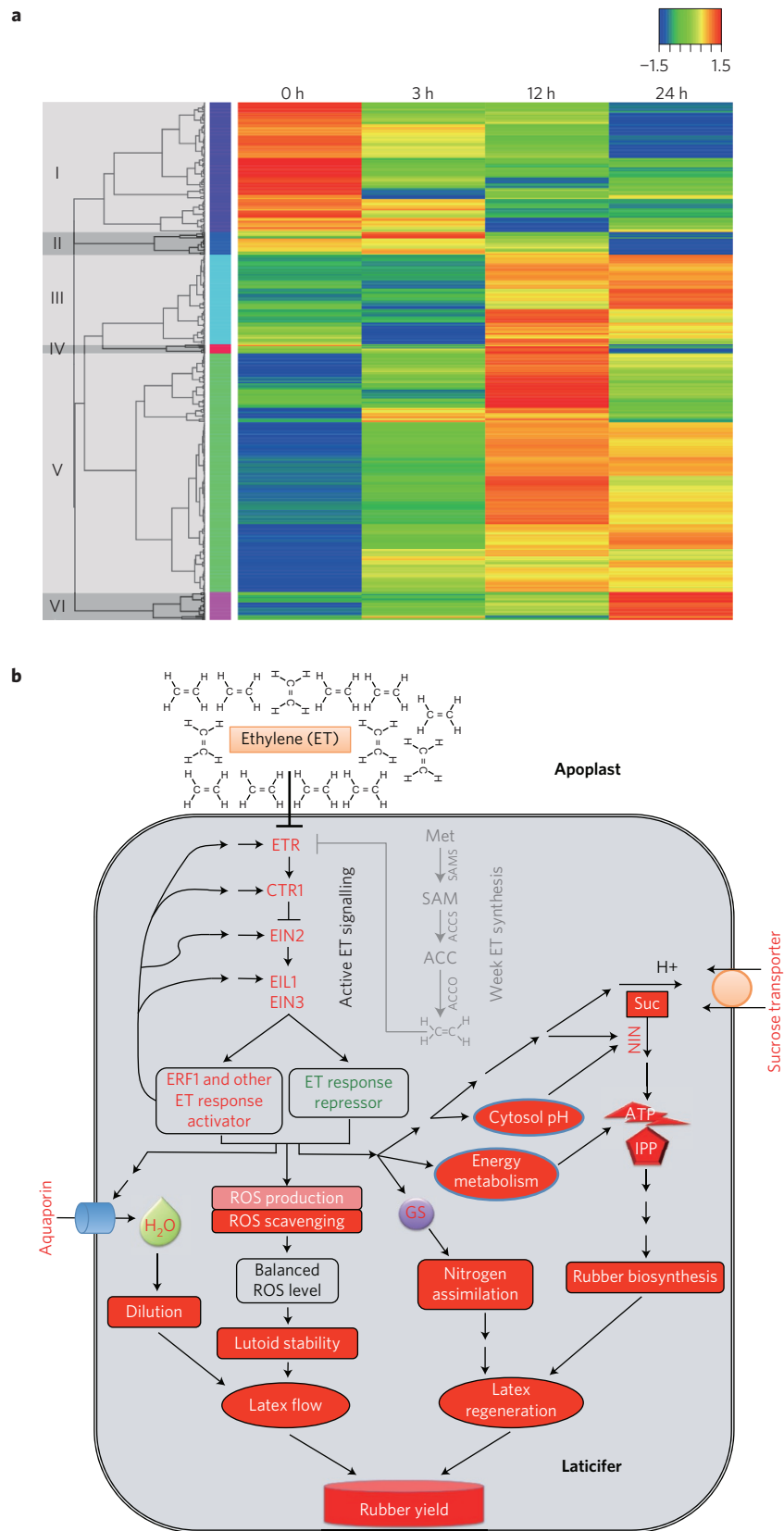


Figure 4 | Ethylene stimulation of rubber production in *Hevea*. **a**, Expression dynamics of differentially expressed genes (DEGs) within 24 h of ethylene treatment. The expression levels (RPKM) of the 509 DEGs are normalized based on the Z-score method (scale bar). The DEGs are divided into six clades; two (clades I and II) of them are downregulated genes whereas the remainder (clades III to VI) are upregulated. **b**, A model summarizing the mechanisms of ethylene stimulation of rubber production. The red and green text used for genes and enzymes denotes that their expression/activity is activated and inhibited by ethylene, respectively. The red background of molecules or events indicates that their quantity or strength is boosted by ethylene; Met, methionine; ROS, reactive oxygen species; NIN, neutral invertase; GS, glutamine synthetase.

and the parallel precursor for *REF1* appear to have evolved from the same ancestral *SRPP* gene, but the emergence of *REF1* was a more recent event (Fig. 3b, upper part of clade 1).

Active ethylene signalling and response in laticifers. Since latex production is greatly increased by the ethylene-releasing agent ethephon, we identified 509 differentially expressed genes (DEGs) in latex that respond to ethylene treatment (Fig. 4a and Supplementary Table 21). About one-quarter of the 342 annotated DEGs (>2-fold expressional change) are transcription factors (53) and protein kinases (31) (Supplementary Tables 22 and 23). Both gene groups are essential in ethylene signal transduction and response in higher plants^{32,33}.

To understand ethylene-dependent mechanisms, we first identified the genes responsible for ethylene biosynthesis in *Hevea* and examined their expression patterns. The three enzymes that act sequentially to synthesize ethylene from methionine, that is S-adenosyl-L-methionine synthase (SAMs), 1-aminocyclopropane-1-carboxylic acid (ACC) synthase (ACS) and ACC oxidase (ACO)³⁴ have 8, 14 and 16 genes respectively in *Hevea* (Supplementary Table 24). However, the expression of these gene families, especially that of SAMs (>fivefold) and ACO (>10-fold) is much lower in latex than other tissues. Such low expression or a lack of expression has been noticed recently for nine ACO genes in *Hevea* latex³⁵. These results, together with the low oxygen condition in latex³⁶ and the requirement of oxygen by ACO to produce ethylene³⁴, point out a weak ethylene-synthesizing ability in laticifers. In addition, ethylene treatment had little effect on the expression of ACS, the rate-limiting enzyme of ethylene biosynthesis in latex (Supplementary Table 24). The primary ethylene signalling components, namely *ETR*, *CTR1*, *EIN2* and *EIN3/EIL1*, were investigated for their expression in latex in response to ethylene treatment (Supplementary Table 25). Four out of the eight receptor genes (*ETR*) showed enhanced expression after ethylene treatment, indicating an ethylene response triggered in laticifers since increased expression has been observed for one or more *ETRs* in every known ethylene response³³. Of particular interest, expressions of two *EIN2s* and one *EIL1* were apparently boosted in latex after ethylene treatment. As the central transducer and master transcription factors in ethylene signalling, *EIN2* and *EIN3/EIL1* genes are mainly controlled by ethylene at a post-translational level^{32,33}. Hitherto, none of these genes identified in other plants has been found to be transcriptionally regulated by ethylene³². The transcriptional enhancement of *EIN2* and *EIL1* in latex suggests an active ethylene signalling in laticifers.

Downstream of the primary ethylene signalling pathway, ethylene-responsive element binding factors (ERFs) are implicated. A total of 225 *Hevea* AP2/ERF members, including 181 ERFs, 35 AP2s, 7 RAVs and 2 Soloists (Supplementary Table 26) were identified, representing the largest assemblage in this grouping as compared to other plants (Supplementary Table 27)³⁷. Nearly one-tenth of the AP2/ERF members showed a more than twofold change in expression after ethylene treatment; 10 of them were upregulated and 11 downregulated (Supplementary Table 28). Interestingly, of the seven downregulated *ERF* genes, four belong to repressor subgroups (ERF-IIa and ERF-VIIIa) of ethylene response³⁸. The depression of their expression is expected to be beneficial for activating downstream ethylene response.

Ethylene treatment triggers a number of stimulated downstream biochemical cascades in relation to latex production: sugar loading and its catabolism^{9,36,39,40}, water uptake⁴¹, energy availability⁴², cytosolic alkalization⁴², nitrogen assimilation⁴³ and defence responses⁴⁴. Many genes implicated in these events were among the DEGs identified in this study (Supplementary Tables 22 and 23), but not the rubber biosynthesis genes, which is consistent with the previous proposition that ethylene has little direct effect on genes in rubber biosynthesis⁴⁵. The defence response genes involved in producing and scavenging reactive oxygen species (ROS) were further analysed

for their importance in the functioning of laticifers²⁰. Three DEGs in ROS production were identified, among which an L-ascorbate oxidase (scaffold2147_8831) and an NADPH oxidase (scaffold0143_441741) appeared upregulated, whereas a lipoxygenase (scaffold4250_5149) was downregulated (Supplementary Tables 22 and 23). Of the six ROS-scavenging DEGs, five that include two thioredoxins (scaffolds0444_166127 and 0520_1896151), a glutaredoxin (scaffold4986_4172), a caleosin-related peroxxygenase (scaffold1473_35058) and polyamine oxidase (scaffold0036_2884533) were upregulated, and one, a thioredoxin (scaffold0794_475278), was downregulated. Both the number of DEGs involved in ROS scavenging and their expression levels after ethylene treatment were much higher than those involved in ROS production. We illustrate in Fig. 4b the mechanisms underlying ethylene stimulation of latex production in *Hevea*.

Discussion

First, an effort to improve genome assembly is especially meaningful in plant genomes with high repeat content⁴⁶. The *Hevea* genome contains 71% repetitive content and our BAC-pool sequencing allowed an over 20-fold increase in scaffold N50 length, which can be exploited in sequencing other repeat-rich large plant genomes. Second, expansion and divergence of the REF/SRPP family and its correlation with rubber biosynthesis leads to new insights into the physiology of rubber-producing laticifers. Third, an in-depth RNA-seq analysis assisted by the high-quality genome assembly has allowed us to gain new understanding of the mechanisms underlying ethylene stimulation of rubber production.

What sets the rubber tree apart from the numerous other rubber-bearing plants⁴⁷ is its ability to produce prodigious amounts of rubber. In this regard, the *Hevea* genome provides a good resource to understand how the tree has managed to accomplish this uncommon feat. An appraisal of data from the genome points to the REF/SRPP gene family, which encompasses the most highly expressed genes in the latex. The divergence of this gene family into several laticifer-specific abundant isoforms suggests extraordinary selection pressure in play. Rubber contained in latex provides *Hevea* with a protective function against boring pests (such as beetles) with its coagulating ability to entrap them in the exuding latex which then self-seals the wound⁴⁸. From the viewpoint of evolutionary advantage to the species, this is the clear benefit that the rubber tree receives. From the anthropological perspective, this adaptation has fortuitous consequences in that it provides mankind with the building blocks of a global industry.

A search for REF and SRPP in the *Hevea* SNP desert is instructive. REF heads the list in gene expression in the SNP desert, implying that it is an active gene that has descended from a recent, single selection of an ancestral sequence. On the other hand, the significance of SRPP in relation to the SNP desert lies in its absence. The phylogenetic dendrogram in Fig. 3b offers an explanation. An SRPP isoform is an ancestral protein in the REF/SRPP gene family. A mutation event occurred relatively recently whereby SRPP was truncated to give rise to REF. Deletion of the SRPP C terminus that resulted in REF isoforms appears to have occurred more than once in the rubber tree's evolutionary history, but the isoforms that prevail in modern *Hevea* are REF1 and SRPP1. The late appearance of REF also explains why, among the other 17 plants examined, the REF/SRPP family has isoform sizes similar to or larger than SRPP1, but none with similar size to REF1. The breakout event that produced REF is important to the modern *Hevea*'s capacity for high rubber production. *Hevea* is unique in its high rubber production arguably because REF is unique to *Hevea*.

There are two classes of rubber particles in *Hevea* latex: the large particles (LRPs) with REF located on their surfaces and the small particles (SRPs) that are coated with SRPP^{25,49}. SRPs are far superior in number, accounting for 94% of all rubber particles in the latex,

whereas LRPs constitute only the remaining 6% of the rubber particles. However, it is precisely this 6% of rubber particles by number that makes up 93% of the rubber by volume in the latex⁵⁰. *REF1* might contribute to rubber biosynthesis by facilitating the biogenesis of LRPs or the 'growing' of SRPs to LRPs. Two pieces of evidence support this presumption: (1) the amount of *REF1* protein in the whole latex has been found to be proportional to the rubber content²⁶; (2) *REF1* gene expression was reported to correlate with yield levels of *Hevea* cultivars²⁷. Taking a hypothetical stance, if *REF* had not evolved to facilitate the formation of LRPs, the typical tapped latex that has a dry rubber content (drc) of 33% would have less than 3% drc for the same number of SRPs per unit volume. In other words, the entire natural rubber industry is essentially founded on a very small proportion of rubber particles that are LRPs.

In *Hevea* planting, the ethylene generating compound, ethephon, is commonly applied to the bark of *Hevea* to lengthen the flow duration and to aid latex regeneration after tapping. Although bearing a weak capability for ethylene synthesis that is little affected by ethylene treatment too, the laticifers reveal an active ethylene signalling capability as evidenced by transcriptional accentuation of the ethylene signal receptor and transduction genes on ethylene stimulation. The low ethylene-synthesizing ability in laticifers, but an active ethylene signalling mechanism that is responsive to exogenous ethylene could shed new light on how ethylene triggers a significant increase in latex flow and rubber production.

The data from this study, together with other public resources, pave a way for whole genome association studies, germplasm improvement and genetic modification of *Hevea* to meet increasing global demand for natural rubber.

Methods

Plant materials. Genomic DNA was prepared from young leaves of six *Hevea* cultivars (Reyan7-33-97, PR107, RRIM600, Reyan8-79, Wenchang11 and Yunyan77-4) (Supplementary Fig. 1) using the CTAB method⁵¹. RNA samples were prepared from mature leaf, male flower, female flower, mature seed, trunk bark, latex and feeder root of ten-year-old mature Reyan7-33-97 trees that had been tapped for two years, or from the latex collected from Reyan7-33-97 trees treated with 1.5% ethephon (2-chloroethylphosphonic acid, an ethylene generator) as described previously³⁹.

Shotgun library construction and sequencing. For genome sequencing, paired-end libraries (<600 bp) were constructed by the standard A-tailing Illumina protocol. Mate-paired libraries (800 bp to 10 kb) were constructed by a modified SOLiD mate-pair library preparation protocol⁵². The Reyan7-33-97 genome was sequenced by the IlluminaGA2 and Hiseq2000 systems, whereas the genomes of re-sequenced cultivars were sequenced solely on the Hiseq2000 platform. Raw reads were preprocessed by an in-house perlscript, and then proofread by the ErrorCorrection module in the SOAPdenovo package⁵³. For RNA-seq, RNA samples were used to prepare libraries and sequenced using the Illumina Hiseq2000 system. Raw RNA-seq reads were processed to trim terminal low quality bases and adapter sequences via an in-house custom pipeline. The clean reads were then mapped to the *Hevea* genome using GSNAP⁵⁴. Cufflinks⁵⁵ was used to compute the transcripts expression levels in reads per kilobase per million reads mapped (RPKM) and to identify the differentially expressed genes (DEGs) upon ethylene stimulation. Hierarchical clustering of DEGs was conducted using custom R scripts.

Genome assembly and validation. The pre-processed paired-end reads were assembled using SOAPdenovo (69-mer size), and mate-pair reads were used to construct scaffolds using SSPACE⁵⁶. Scaffold gaps were closed with Gapfiller⁵⁷ and the cd-hit software was employed to filter chimeric scaffolds⁵⁸. A BAC-pooling sequencing strategy was employed to improve the assembly further (Supplementary Fig. 4 and Supplementary Note 1). Public databases, BAC and transcript sequences were used to validate the genome assembly (Supplementary Note 4).

Genome annotation. Genome repeat sequences were annotated *de novo* by using RepeatMasker (<http://www.repeatmasker.org>). The protein-coding genes were predicted based on the repeat-masked genome through a combination of *ab initio*, conserved protein homologues and assembled transcripts. The non-coding RNAs were annotated by employing the INFERNAL software⁵⁹ to search against the Rfam database (Supplementary Note 5).

Estimation of whole-genome duplication. The all-to-all BLASTP program was used to identify the homolog pairs in *Hevea* proteins and the MCScan program⁶⁰ was used to

search for collinearity blocks which were then filtered using the criterion of fewer than ten non-collinear genes between any two collinear genes. The same method was used to identify the syntenic blocks in *L. usitatissimum*, *P. trichocarpa*, *R. communis* and *M. esculenta*, or between *Hevea* and any of the four species. The collinearity region sizes for *Hevea*, *M. esculenta* and *P. trichocarpa* were estimated statistically by the Wilcoxon test. To estimate the duplication event, we calculated the synonymous K_2 and fourfold synonymous third-codon transversion position (4DTV) using KaKs_calculator⁶¹ with the NG model and an in-house perl script, respectively.

Phylogenetic analysis. Twelve species, *Medicago truncatula*, *Glycine max*, *Fragaria vesca*, *Vitis vinifera*, *Oryza sativa*, *L. usitatissimum*, *P. trichocarpa*, *R. communis*, *M. esculenta*, *Citrus sinensis*, *Carica papaya* and *Arabidopsis thaliana*, were selected to construct a phylogenetic tree with *Hevea* using 72 single-copy gene families (Supplementary Note 7). These species represent the typical Rosids sequenced to date in the Eudicots. *O. sativa* was designated as an outgroup.

Genetic heterogeneity of *Hevea* cultivars. Paired-end sequences (35×) from each of the six *Hevea* cultivars were mapped to the Reyan7-33-97 reference genome using BWA (ref. 62). The mapping results were transformed into bam format and sorted with SAMtools⁶³. SNP calling results were filtered against the following criteria: (1) each SNP supported by at least five non-redundant reads; (2) average mapping quality more than 40; and (3) two SNPs within 10 bp to be excluded. Based on the SNP calling results, SNP deserts (<1 SNP per kb) were identified in each sequenced cultivar using a perl script. Genes located in SNP deserts were subjected to functional annotation and GO enrichment analysis using GOEAST (<http://omicslab.genetics.ac.cn/GOEAST/>).

Genes associated with rubber biosynthesis, ethylene synthesis and signalling. The 20 gene families that have been reported as involved in rubber biosynthesis were identified from the genome (Supplementary Note 10). Ethylene synthesis and signalling genes that had been characterized in *A. thaliana*⁶⁴ were retrieved for their corresponding protein sequences from the Arabidopsis Information Resource (TAIR) (<https://www.arabidopsis.org/index.jsp>). The retrieved *A. thaliana* proteins were processed with Interproscan⁶⁵ and Blastp searched against *Hevea* proteins. Hits sharing >30% amino acid identity and >50% amino acid alignment length with the *A. thaliana* homologues were further checked for pfam domain architecture. Those having the same pfam domains as their *A. thaliana* homologues were regarded as proteins involved in ethylene synthesis and signalling in *Hevea* (Supplementary Table 25).

The *H. brasiliensis* genome and RNA-seq sequences have been deposited in GenBank/DBJ/EMBL under the accession codes of LVXX01000000 and SRP069104, respectively.

Received 13 February 2016; accepted 22 April 2016;
published online 23 May 2016

References

- van Beilen, J. B. & Poirier, Y. Establishment of new crops for the production of natural rubber. *Trends Biotechnol.* **25**, 522–529 (2007).
- Jones, K. Natural rubber as a green commodity—Part II. *Rubber Dev.* **47**, 37–41 (1994).
- Chan, H. in *Milestones in Rubber Research* (ed. Ong, E. L.) 2–15 (Malaysian Rubber Board, 2000).
- Priyadarshan, P. & Goncalves, P. d.S. *Hevea* gene pool for breeding. *Genet. Resour. Crop Ev.* **50**, 101–114 (2003).
- Paardekooper, E. in *Rubber* (eds Webster, C. & Baulkwill, W.) 349–414 (Longman Scientific and Technical, 1989).
- Clément-Demange, A., Priyadarshan, P., Hoa, T. T. T. & Venkatachalam, P. *Hevea* rubber breeding and genetics. *Plant Breeding Rev.* **29**, 177 (2007).
- Rahman, A. Y. et al. Draft genome sequence of the rubber tree *Hevea brasiliensis*. *BMC Genomics* **14**, 75 (2013).
- Wang, X. et al. Comprehensive proteomics analysis of laticifer latex reveals new insights into ethylene stimulation of natural rubber production. *Sci. Rep.* **5**, 13778 (2015).
- Liu, J. P., Xia, Z. Q., Tian, X. Y. & Li, Y. J. Transcriptome sequencing and analysis of rubber tree (*Hevea brasiliensis* Muell.) to discover putative genes associated with tapping panel dryness (TPD). *BMC Genomics* **16**, 398 (2015).
- Hurtado Paez, U. A., Garcia Romero, I. A., Restrepo Restrepo, S., Aristizabal Gutierrez, F. A. & Montoya Castano, D. Assembly and analysis of differential transcriptome responses of *Hevea brasiliensis* on interaction with *Microcyclus ulei*. *PLoS ONE* **10**, e0134837 (2015).
- Chao, J., Chen, Y., Wu, S. & Tian, W. M. Comparative transcriptome analysis of latex from rubber tree clone CATAS8-79 and PR107 reveals new cues for the regulation of latex regeneration and duration of latex flow. *BMC Plant Biol.* **15**, 104 (2015).
- Wang, S., Xu, Y., Luo, S. & Gao, X. Adaptability of new desirable rubber clone Reyan7-33-97 in central mountainous areas of Hainan province. *Chin. J. Trop. Agr.* **29**, 1–4 (2009).
- Huang, H., Liang, M., Wu, Y., Li, D. & He, J. Selection and breeding of a moderate scale clone SCATC7-33-97. *Chin. J. Trop. Crops* **15**, 1–6 (1994).

14. Xi, Z. *et al.* Phylogenomics and a posteriori data partitioning resolve the Cretaceous angiosperm radiation Malpighiales. *Proc. Natl Acad. Sci. USA* **109**, 17519–17524 (2012).
15. Sun, M. *et al.* Deep phylogenetic incongruence in the angiosperm clade Rosidae. *Mol. Phylogenet. Evol.* **83**, 156–166 (2015).
16. Kaplan, N. L., Hudson, R. & Langley, C. The “hitchhiking effect” revisited. *Genetics* **123**, 887–899 (1989).
17. Wang, L. *et al.* SNP deserts of Asian cultivated rice: genomic regions under domestication. *J. Evol. Biol.* **22**, 751–761 (2009).
18. Tenaillon, M. I., U’Ren, J., Tenaillon, O. & Gaut, B. S. Selection versus demography: a multilocus investigation of the domestication process in maize. *Mol. Biol. Evol.* **21**, 1214–1225 (2004).
19. Al-Mssallem, I. S. *et al.* Genome sequence of the date palm *Phoenix dactylifera* L. *Nature Commun.* **4**, 2274 (2013).
20. d’Auzac, J. *et al.* The regulation of cis-polyisoprene production (natural rubber) from *Hevea brasiliensis*. *Recent Res. Dev. Plant Physiol.* **1**, 273–332 (1997).
21. Chow, K. S. *et al.* Insights into rubber biosynthesis from transcriptome analysis of *Hevea brasiliensis* latex. *J. Exp. Bot.* **58**, 2429–2440 (2007).
22. Sando, T. *et al.* Cloning and characterization of the 2-C-methyl-D-erythritol 4-phosphate (MEP) pathway genes of a natural-rubber producing plant, *Hevea brasiliensis*. *Biosci. Biotech. Bioch.* **72**, 2903–2917 (2008).
23. Sando, T. *et al.* Cloning and characterization of mevalonate pathway genes in a natural rubber producing plant, *Hevea brasiliensis*. *Biosci. Biotech. Bioch.* **72**, 2049–2060 (2008).
24. Epping, J. *et al.* A rubber transferase activator is necessary for natural rubber biosynthesis in dandelion. *Nature Plants* **1**, 15048 (2015).
25. Oh, S. K. *et al.* Isolation, characterization, and functional analysis of a novel cDNA clone encoding a small rubber particle protein from *Hevea brasiliensis*. *J. Biol. Chem.* **274**, 17132–17138 (1999).
26. Dennis, M. S. & Light, D. R. Rubber elongation factor from *Hevea brasiliensis*. Identification, characterization, and role in rubber biosynthesis. *J. Biol. Chem.* **264**, 18608–18617 (1989).
27. Priya, P., Venkatachalam, P. & Thulaseedharan, A. Differential expression pattern of rubber elongation factor (REF) mRNA transcripts from high and low yielding clones of rubber tree (*Hevea brasiliensis* Muell. Arg.). *Plant Cell Rep.* **26**, 1833–1838 (2007).
28. Hillebrand, A. *et al.* Down-regulation of small rubber particle protein expression affects integrity of rubber particles and rubber content in *Taraxacum brevicorniculatum*. *PLoS ONE* **7**, e41874 (2012).
29. Laibach, N., Hillebrand, A., Twyman, R. M., Pruffer, D. & Schulze Gronover, C. Identification of a *Taraxacum brevicorniculatum* rubber elongation factor protein that is localized on rubber particles and promotes rubber biosynthesis. *Plant J.* **82**, 609–620 (2015).
30. Berthelot, K. *et al.* Rubber elongation factor (REF), a major allergen component in *Hevea brasiliensis* latex has amyloid properties. *PLoS ONE* **7**, e48065 (2012).
31. Gidda, S. K. *et al.* Lipid droplet-associated proteins (LDAPs) are involved in the compartmentalization of lipophilic compounds in plant cells. *Plant Signal. Behav.* **8**, e27141 (2013).
32. Yang, C., Lu, X., Ma, B., Chen, S. Y. & Zhang, J. S. Ethylene signaling in rice and *Arabidopsis*: conserved and diverged aspects. *Mol. Plant* **8**, 495–505 (2015).
33. Klee, H. J. Ethylene signal transduction. Moving beyond *Arabidopsis*. *Plant Physiol.* **135**, 660–667 (2004).
34. Yang, S. F. & Hoffman, N. E. Ethylene biosynthesis and its regulation in higher plants. *Ann. Rev. Plant Physiol.* **35**, 155–189 (1984).
35. Zhu, J. H., Xu, J., Chang, W. J. & Zhang, Z. L. Isolation and molecular characterization of 1-aminocyclopropane-1-carboxylic acid synthase genes in *Hevea brasiliensis*. *Int. J. Mol. Sci.* **16**, 4136–4149 (2015).
36. Tupy, J. in *Physiology of Rubber Tree Latex* (eds d’Auzac, J., Jacob, J.-L. & Chrestin, H.) 179–218 (CRC, 1989).
37. Piyatrakul, P. *et al.* Sequence and expression analyses of ethylene response factors highly expressed in latex cells from *Hevea brasiliensis*. *PLoS ONE* **9**, e99367 (2014).
38. Nakano, T., Suzuki, K., Fujimura, T. & Shinshi, H. Genome-wide analysis of the ERF gene family in *Arabidopsis* and rice. *Plant Physiol.* **140**, 411–432 (2006).
39. Tang, C. *et al.* The sucrose transporter HbSUT3 plays an active role in sucrose loading to laticifer and rubber productivity in exploited trees of *Hevea brasiliensis* (para rubber tree). *Plant Cell Environ.* **33**, 1708–1720 (2010).
40. Dusotoit-Coucaud, A. *et al.* Ethylene stimulation of latex yield depends on the expression of a sucrose transporter (HbSUT1B) in rubber tree (*Hevea brasiliensis*). *Tree Physiol.* **30**, 1586–1598 (2010).
41. Tungngoen, K. *et al.* Involvement of HbPIP2;1 and HbTIP1;1 aquaporins in ethylene stimulation of latex yield through regulation of water exchanges between inner liber and latex cells in *Hevea brasiliensis*. *Plant Physiol.* **151**, 843–856 (2009).
42. Amalou, Z., Bangratz, J. & Chrestin, H. Ethrel (ethylene releaser)-induced increases in the adenylate pool and transtonoplast delta pH within *Hevea* latex cells. *Plant Physiol.* **98**, 1270–1276 (1992).
43. Pujade-Renaud, V. *et al.* Ethylene-Induced increase in glutamine synthetase activity and mRNA levels in *Hevea brasiliensis* latex cells. *Plant Physiol.* **105**, 127–132 (1994).
44. Putranto, R. A. *et al.* Ethylene response factors are controlled by multiple harvesting stresses in *Hevea brasiliensis*. *PLoS ONE* **10**, e0123618 (2015).
45. Zhu, J. & Zhang, Z. Ethylene stimulation of latex production in *Hevea brasiliensis*. *Plant Signal. Behav.* **4**, 1072–1074 (2009).
46. Feuillet, C., Leach, J. E., Rogers, J., Schnable, P. S. & Eversole, K. Crop genome sequencing: lessons and rationales. *Trends Plant Sci.* **16**, 77–88 (2011).
47. Polhamus, L. G. *Rubber*. (Leonard Hill, London, 1962).
48. Sharples, A. The laticiferous system of *Hevea brasiliensis* and its protective function. *Ann. Bot.* **32**, 247–251 (1918).
49. Berthelot, K. *et al.* Rubber particle proteins, HbREF and HbSRPP, show different interactions with model membranes. *BBA-Biomembranes* **1838**, 287–299 (2014).
50. Yeang, H., Yip, E. & Hamzah, S. Characterisation of Zone 1 and Zone 2 rubber particles in *Hevea brasiliensis* latex. *J. Nat. Rubb. Res.* **10**, 108–123 (1995).
51. Allen, G. C., Flores-Vergara, M. A., Krasynanski, S., Kumar, S. & Thompson, W. F. A modified protocol for rapid DNA isolation from plant tissues using cetyltrimethylammonium bromide. *Nature Protoc.* **1**, 2320–2325 (2006).
52. van Heesch, S. *et al.* Improving mammalian genome scaffolding using large insert mate-pair next-generation sequencing. *BMC Genomics* **14**, 257 (2013).
53. Li, R. *et al.* De novo assembly of human genomes with massively parallel short read sequencing. *Genome Res.* **20**, 265–272 (2010).
54. Wu, T. D. & Nacu, S. Fast and SNP-tolerant detection of complex variants and splicing in short reads. *Bioinformatics* **26**, 873–881 (2010).
55. Trapnell, C. *et al.* Differential gene and transcript expression analysis of RNA-seq experiments with TopHat and Cufflinks. *Nature Protoc.* **7**, 562–578 (2012).
56. Boetzer, M., Henkel, C. V., Jansen, H. J., Butler, D. & Pirovano, W. Scaffolding pre-assembled contigs using SSPACE. *Bioinformatics* **27**, 578–579 (2011).
57. Nadalin, F., Vezzi, F. & Policriti, A. GapFiller: a de novo assembly approach to fill the gap within paired reads. *BMC Bioinformatics* **13** (Suppl. 14), S8 (2012).
58. Fu, L., Niu, B., Zhu, Z., Wu, S. & Li, W. CD-HIT accelerated for clustering the next-generation sequencing data. *Bioinformatics* **28**, 3150–3152 (2012).
59. Nawrocki, E. P. & Eddy, S. R. Infernal 1.1: 100-fold faster RNA homology searches. *Bioinformatics* **29**, 2933–2935 (2013).
60. Tang, H. *et al.* Synteny and collinearity in plant genomes. *Science* **320**, 486–488 (2008).
61. Zhang, Z. *et al.* KaKs_Calculator: calculating Ka and Ks through model selection and model averaging. *Genomics Proteomics Bioinformatics* **4**, 259–263 (2006).
62. Li, H. & Durbin, R. Fast and accurate short read alignment with Burrows-Wheeler transform. *Bioinformatics* **25**, 1754–1760 (2009).
63. Li, H. *et al.* The Sequence Alignment/Map format and SAMtools. *Bioinformatics* **25**, 2078–2079 (2009).
64. Zhao, Q. & Guo, H. W. Paradigms and paradox in the ethylene signaling pathway and interaction network. *Mol. Plant* **4**, 626–634 (2011).
65. Li, W. *et al.* The EMBL-EBI bioinformatics web and programmatic tools framework. *Nucleic Acids Res.* **43**, W580–W584 (2015).

Acknowledgements

We thank E. (Liansheng) Zheng for critically reading the manuscript. This research was financially supported by grants from the Fundamental Research Funds for Rubber Research Institute, CATAS, and the 863 program (2013AA102605).

Author contributions

H.H. and C.T. conceptualized the research programme. C.T., S.H., H.H. and J.Y. designed experiments and coordinated the project. C.T. and S.H. supervised the data generation and analysis. M.Y., Y.F., C.T., Y.L., S.H.G. and H.M. performed most of the data analysis. B.Z. and X.T. organized the experiments for genome- and BAC- sequencing, RNA-seq and library construction. X.X., B.Z., Z.A., Y.Q., J.H.Y., X.L., J.Q. and Y.H. performed the field experiments, DNA and RNA extraction, and PCR amplification for target genes. Q.L., P.M., Z.H., M.S., W.J.L., X.Z., H.C., Y.L., J.Y., W.T., N.Z., R.Z.Z., D.L., P.H., Z.L., Z.Z., S.L., C.L., J.W., D.W., C.Q.L. and W.L. were partially involved in either experiments or data analysis. C.T., M.Y., Y.F., H.Y., J.Y. and S.H. wrote the manuscript. All authors discussed results and commented on the manuscript.

Additional information

Supplementary information is available [online](http://www.nature.com/online). Reprints and permissions information is available [online](http://www.nature.com/reprints) at www.nature.com/reprints. Correspondence and requests for materials should be addressed to C.T. and S.H.

Competing interests

The authors declare no competing financial interests.



This work is licensed under a Creative Commons Attribution 4.0 International License. The images or other third party material in this article are included in the article's Creative Commons license, unless indicated otherwise in the credit line; if the material is not included under the Creative Commons license, users will need to obtain permission from the license holder to reproduce the material. To view a copy of this license, visit <http://creativecommons.org/licenses/by/4.0/>